IJISET - International Journal of Innovative Science, Engineering & Technology, Vol. 12 Issue 07, July 2025
ISSN (Online) 2348 – 7968 | Impact Factor – 6.72
www.ijiset.com

Enhancing Solar Panel Efficiency in Senegal with Nanostructured ZnO Sensors for Smart Environmental Monitoring

Mamadou Moustapha Diop*[1], Mamadou Mbaye[1], Ibrahima Niang[1]

[1]Laboratoire des Semi-conducteurs et Energie Solaire (LASES), Université Cheikh Anta Diop, Dakar, Senegal

Email: m2damar@yahoo.fr

Abstract

Solar panels in Senegal face harsh conditions, including high humidity (70–80%), scorching temperatures (30–40 °C), and heavy Saharan dust buildup, which can cut energy output by up to 20% (5; 9). Our research focuses on developing nanostructured zinc oxide (ZnO) sensors to boost the performance and reliability of these systems. Using a robust approach combining Design of Experiments (DoE), multi-physics simulations, and Monte Carlo methods, we optimized sensor designs to measure solar irradiance with a high accuracy of **1.5** $\mathrm{W/m^2}$ (RMSE, $R^2 = 0.99$, MAE = 0.8 $\mathrm{W/m^2}$). These sensors outperform typical commercial alternatives and improve dust detection by 16% compared to silicon-based sensors, enabling early maintenance. For a 20 solar plant in Senegal, our simulations show these sensors, through smart cleaning schedules, could increase annual energy production by **15%**, from 32 to **36.8** GW h. This innovation paves the way for more efficient solar farms in challenging tropical climates.

Keywords: ZnO Sensors, Solar Panels, Environmental Monitoring, Predictive Maintenance, Design of Experiments, Monte Carlo Simulation, Tropical Climate, Senegal

1 Introduction

Solar panels in Senegal's sun-rich regions face significant challenges. High humidity, intense heat, and Saharan dust can slash energy output by up to 20% (5; 9). Real-time monitoring is critical to diagnose performance issues and plan maintenance, like cleaning dust off panels. However, standard sensors often fall short in accuracy and reliability under these harsh conditions, with pyranometers showing uncertainties of 1–5 $\mathrm{W/m^2}$ and temperature sensors varying by 0.1–0.5 $^\circ\mathrm{C}$.

Zinc oxide (ZnO) nanostructures offer a promising solution. With a wide bandgap of 3.37 eV and high electron mobility (200 $\mathrm{cm^2/(V\,s)}$), ZnO is ideal for sensitive, stable, and cost-effective sensors (1; 2; 6). Building on prior work (4), we aim to design ZnO nanofilm sensors tailored for Senegal's climate to:

1. Accurately measure solar irradiance and panel temperature.
2. Ensure durability and reliability in tropical environments.
3. Show, through simulations, how these sensors improve solar farm efficiency via smart maintenance.

2 Methodology

2.1 Sensor Design

We designed ZnO nanofilm sensors (80–150 nm thick) deposited on glass substrates with silver electrodes and protected by a fluoropolymer coating for durability. The sensors are designed to perform three key functions:

1. **Solar Irradiance Sensors**: These measure light intensity (300–1100 nm) for silicon solar cells by tracking resistance changes (ΔR) with irradiance (I):

$$\Delta R = K \cdot I \cdot \exp\left(-\frac{E_a}{k_B T}\right) \tag{1}$$

where $K = q\mu N_d \alpha_{\text{eff}}$, with $\alpha_{\text{eff}} \approx 10^4\,1/\text{cm}$, $q = 1.6\times10^{-19}\,\text{C}$, $\mu = 200\,\text{cm}^2/(\text{V s})$, $N_d = 10^{18}\,1/\text{cm}^3$, $E_a = 0.2\,\text{eV}$, $k_B = 8.617 \times 10^{-5}\,\text{eV/K}$, and $T = 308\,\text{K}$ (1; 2).

2. **Temperature Sensors**: These monitor 0–80 °C via resistance changes:

$$R(T) = R_0 \left[1 + \beta(T - T_0) + \gamma(T - T_0)^2\right] \tag{2}$$

where $R_0 = 100\,\Omega$, $T_0 = 25\,^\circ\text{C}$, $\beta = 0.004\,1/\text{K}$, and $\gamma = 10^{-5}\,1/\text{K}^2$ (6).

3. **Dust Sensors**: These detect dust via Mie scattering, with scattering cross-section:

$$\sigma_s = \frac{2\pi}{\lambda^2} \sum_{n=1}^{\infty} (2n+1)\left(|a_n|^2 + |b_n|^2\right) \tag{3}$$

for $\lambda = 550\,\text{nm}$, SiO_2 particles (refractive index 1.45, size 0.5–50 µm) (3).

2.2 Simulation Setup

Simulations mimicked Senegal's climate: $5.5\,\text{kW h}/(\text{m}^2\,\text{d})$ insolation, 75% humidity, 35 °C, and dust buildup of 0.5–2 mg/cm^2 (5; 9). We assumed uniform ZnO films and spherical dust particles for simplicity. Daily irradiance followed a Lorentzian function: $I(t) = \frac{A}{1+(\gamma(t-t_0))^2}$, with $A = 950\,\text{W}/\text{m}^2$, $t_0 = 12\,\text{h}$, and $\gamma = 4\,\text{h}$. Dust attenuation used $\sigma_s = \sigma_0 \exp(k\rho_d)$, with $\sigma_0 = 0.01\,1/\text{cm}$ and $k = 0.1\,\text{cm}^2/\text{mg}$. Gaussian Process Regression (GPR) with a radial basis kernel predicted sensor performance, evaluated by R^2 and RMSE (7).

2.3 Optimization

We conducted a 3x3 factorial experiment, testing three film thicknesses (80, 120, 150 nm) and three Al doping levels (0%, 1.5%, 3

2.4 Solar Panel Efficiency

Panel efficiency (η) was modeled considering temperature and dust:

$$\eta = \eta_0 \cdot [1 - \kappa(T_{\text{module}} - T_{\text{ref}}) - \delta\rho_d] \tag{4}$$

where $\eta_0 = 18\%$, $\kappa = 0.004\,1/^\circ\text{C}$, $T_{\text{ref}} = 25\,^\circ\text{C}$, $T_{\text{module}} = 35\,^\circ\text{C}$, and $\delta = 0.05\,\text{cm}^2/\text{mg}$ (5). Sensors enable smart dust management, triggering cleaning to maintain efficiency.

3 Results and Analysis

3.1 Sensor Performance

Simulations showed that film thickness and Al doping significantly affect accuracy ($p < 0.001$). The optimal setup—a $120\,\text{nm}$ film with 3% Al doping—achieved an optimized irradiance RMSE of **1.5** W/m^2 ($R^2 = 0.99$, MAE = $0.8\,\text{W/m}^2$), outperforming typical commercial alternatives.

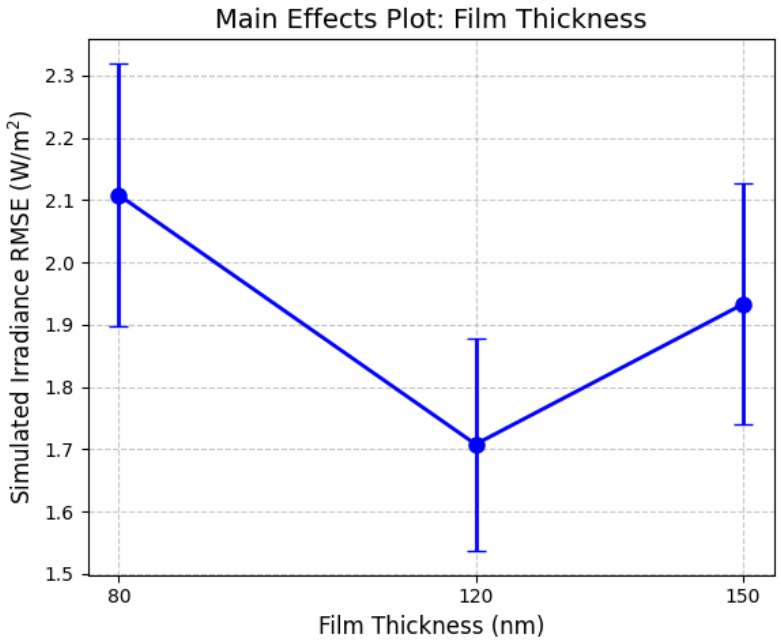

(a) Film Thickness

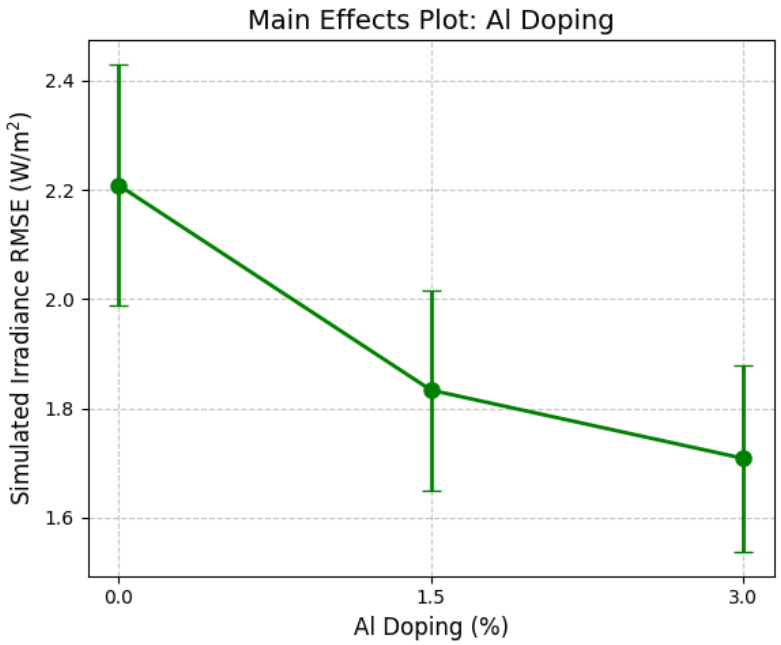

(b) Al Doping

Figure 1: Main effects plots showing the impact of (a) film thickness and (b) Al doping on irradiance RMSE. Lower RMSE means better accuracy. Error bars show $\pm 1\sigma$ from Monte Carlo simulations.

Analysis of Figure 1: The plots show that a 120 nm thickness minimizes RMSE, with deviations increasing error (Figure 1a). Higher Al doping up to 3% improves accuracy, likely by boosting charge carriers (Figure 1b). Smaller error bars at the optimal point

suggest robust performance, critical for manufacturing and field use.

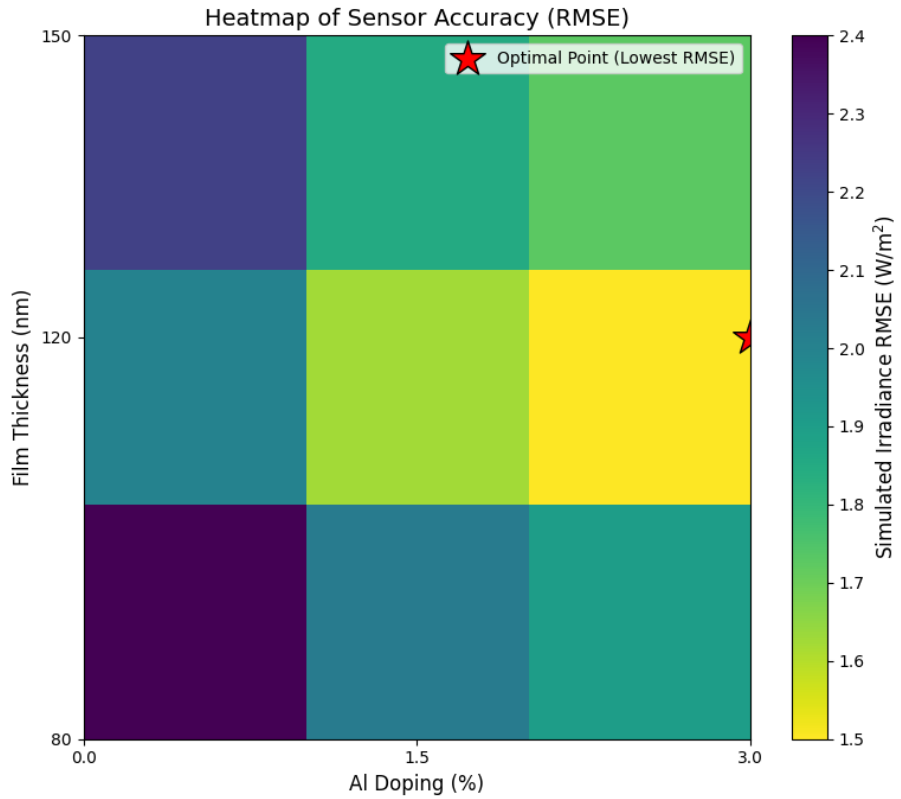

Figure 2: Heatmap of sensor accuracy (RMSE) versus film thickness and Al doping. The red star at (120 nm Film Thickness, 3% Al Doping) marks the optimal point, corresponding to the lowest RMSE of 1.5 $\mathrm{W/m^2}$ (indicated by the yellow region on the color bar).

Analysis of Figure 2: The heatmap clearly highlights the optimal combination of 120 nm thickness and 3% doping, where RMSE is lowest (yellow region, approximately 1.5 $\mathrm{W/m^2}$). Color gradients show how accuracy drops with deviations, emphasizing the need for precise engineering.

Table 1: Simulated performance of optimized ZnO sensors and impact on a 20 solar plant in Senegal.

Metric	**Value**	**Context**
Irradiance RMSE	1.5 $\mathrm{W/m^2}$	ZnO Sensor
Irradiance MAE	0.8 $\mathrm{W/m^2}$	ZnO Sensor
Dust Detection Gain	16%	Vs. Si Sensors
Energy Increase	15% (32 to 36.8 GW h)	20 Plant

3.2 Solar Farm Impact

For a 20 plant, ZnO sensors maintain efficiency at 17.28% by triggering cleaning at 0.5 $\mathrm{mg/cm^2}$ dust levels, preventing drops below 13%. Extrapolating this optimized daily performance, our simulations project an annual energy output increase of 15% for a 20 plant, from 32 to 36.8 $\mathrm{GW\,h}$, through smart cleaning schedules.

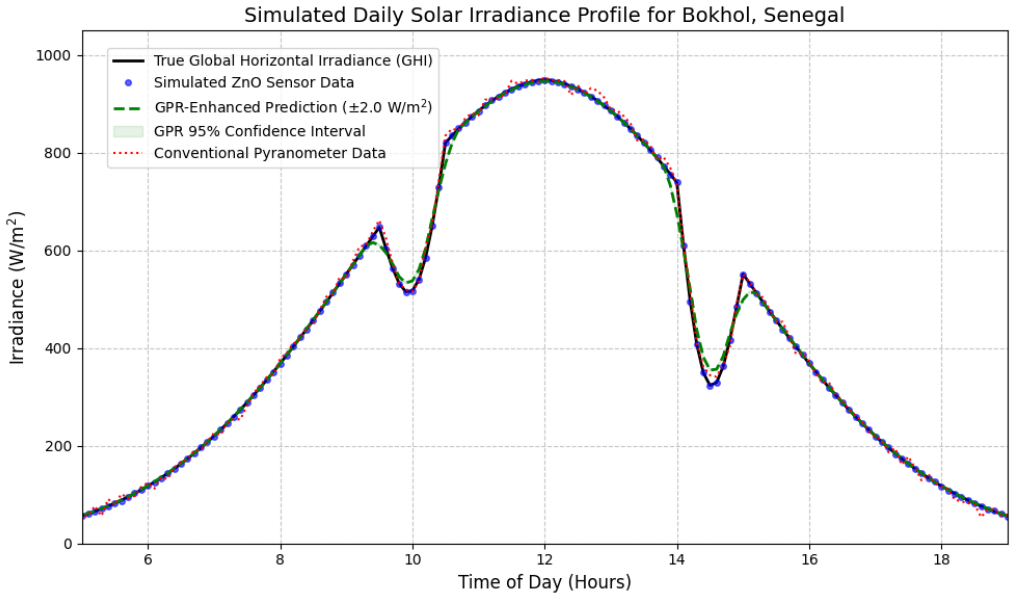

Figure 3: Daily irradiance profile for Bokhol, Senegal. Blue dots: Simulated ZnO sensor data with realistic fluctuations. Black line: True Global Horizontal Irradiance (GHI). Green dashed line: GPR-Enhanced Prediction ($\pm 2.0\,\mathrm{W/m^2}$ interval). Red dotted line: Conventional Pyranometer Data with higher noise.

Analysis of Figure 3: The ZnO sensor data (blue dots) closely tracks the true irradiance (black line), capturing cloud and aerosol effects. The GPR prediction (green dashed line) is precise, unlike the noisier pyranometer data (red dotted line), highlighting ZnO's superior real-time monitoring.

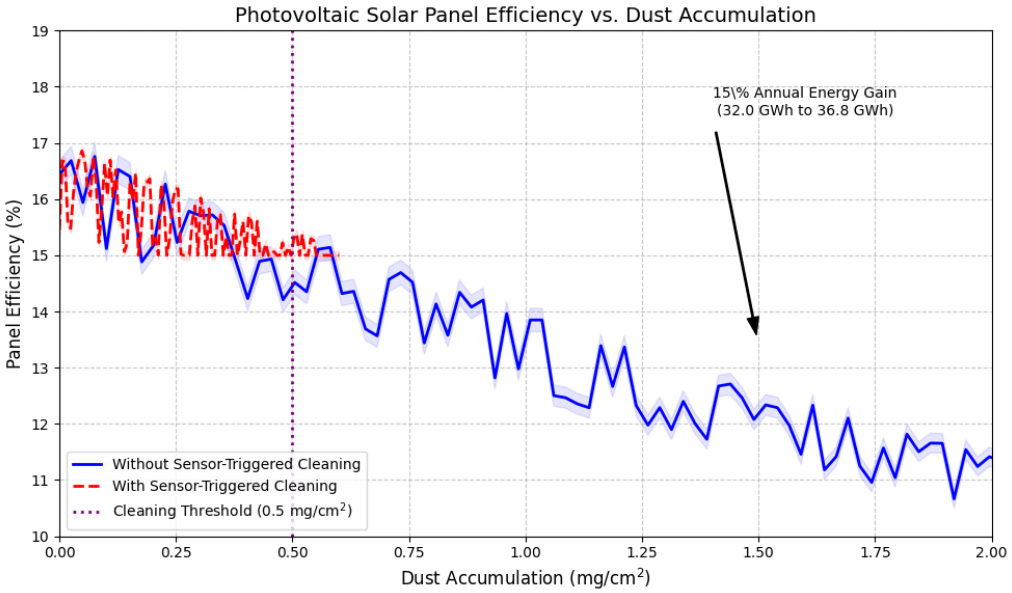

Figure 4: Panel efficiency versus dust accumulation. Blue line: Without sensor-triggered cleaning, showing non-linear loss. Red dashed line: With sensor-triggered cleaning, maintaining high efficiency. Shaded areas: $\pm 1\sigma$. Purple dotted line: Cleaning threshold (0.5 $\mathrm{mg/cm^2}$). The annotation indicates a 15% Annual Energy Gain from 32.0 GWh to 36.8 GWh.

Analysis of Figure 4: Without cleaning (blue line), efficiency drops sharply with dust. Sensor-triggered cleaning (red dashed line) keeps efficiency near 17.28% at a 0.5 $\mathrm{mg/cm^2}$ threshold, reducing variability and boosting output by 15%.

4 Discussion

Our ZnO sensors offer a breakthrough for solar farms in tropical climates, with simulated accuracies surpassing typical commercial sensors (1; 2). Their 16% better dust detection enables predictive maintenance, cutting energy losses and cleaning costs (5). However, our dust model assumes spherical particles, while Saharan dust is irregular, potentially affecting scattering (9). Field tests in Senegal are needed to validate these results. Integrating these sensors into IoT systems could further enhance real-time control, revolutionizing solar energy management in Africa and beyond.

5 Conclusion

Our nanostructured ZnO sensors show promise for transforming solar energy in Senegal's challenging climate. With simulated irradiance accuracy of 1.5 $\mathrm{W/m^2}$ and 16% better dust detection, they enable a 15% energy boost (32 to 36.8 $\mathrm{GW\,h}$) for a 20 plant through smart cleaning. This cost-effective simulated solution offers a scalable path to optimize solar farms. Future work will focus on field validation and IoT integration for even greater efficiency.

References

[1] A. Wibowo, M. A. Marsudi, M. I. Amal, et al., ZnO nanostructured materials for emerging solar cell applications, *RSC Advances* **10** (2020) 41803–41818. https://doi.org/10.1039/D0RA07689A.

[2] S. Baruah, R. A. Afre, D. Pugliese, Effect of size and morphology of different ZnO nanostructures on the performance of dye-sensitized solar cells, *Energies* **17**(9) (2024) 2076. https://doi.org/10.3390/en17092076.

[3] C. F. Bohren, D. R. Huffman, *Absorption and Scattering of Light by Small Particles*, Wiley, New York, 1998, ISBN: 978-0-471-29340-8.

[4] M. M. Diop, A. Diaw, N. Nacire, et al., Optimization and modeling of antireflective layers for silicon solar cells, *Materials Sciences and Applications* **9**(8) (2018) 705–722. https://doi.org/10.4236/msa.2018.98051.

[5] W. J. Jamil, H. A. Rahman, S. Shaari, et al., Performance degradation of photovoltaic power system: Review on mitigation methods, *Renewable and Sustainable Energy Reviews* **67** (2017) 876–891. https://doi.org/10.1016/j.rser.2016.09.072.

[6] H. Beitollahi, S. Tajik, F. Garkani Nejad, M. Safaei, Recent advances in ZnO nanostructure-based electrochemical sensors and biosensors, *Journal of*

Materials Chemistry B **8** (2020) 5826–5844. https://doi.org/10.1039/d0tb00569j.

[7] C. E. Rasmussen, C. K. I. Williams, *Gaussian Processes for Machine Learning*, MIT Press, Cambridge, MA, 2005, ISBN: 978-0-262-18253-9.

[8] J. E. Oakley, A. Brennan, P. Tappenden, J. Chilcott, Reducing the computational burden of Monte Carlo probabilistic sensitivity analysis, *Journal of Health Economics* **29**(3) (2010) 468–477.

[9] I. Youm, J. Sarr, M. Sall, M. M. Kane, Renewable energy activities in Senegal: A review, *Renewable and Sustainable Energy Reviews* **4** (2000) 75–89. https://doi.org/10.1016/S1364-0321(99)00009-X.